ISSN 0029-3865

CBPF-NF-042/87

COMPARISON OF MODELS FOR REASSOCIATION OF CO WITH CARP HEMOGLOBIN

by

Lêa J. El-Jaick*, Eliane Wajnberg, George Bemski
and Marilia P. Linhares[1]

Centro Brasileiro de Pesquisas Físicas - CNPq/CBPF
Rua Dr. Xavier Sigaud, 150
22290 - Rio de Janeiro, RJ - Brasil

[1]Universidade Federal do Rio de Janeiro
Instituto de Física
Cidade Universitária
21910 - Rio de Janeiro, RJ - Brasil

*To whom correspondence should be addressed.

ABSTRACT

A comparison among three models[4-6] for reassociation of CO with carp-hemoglobin, in R state, is made for temperatures below 200K. The experimental data utilized are from Cobau et al.[7] who analyzed them according to one of these models. The differences among the models lead to distinct shapes of their energy distributions. Nevertheless it was verified that the peak energy of these distributions and the Arrhenius frequency factor are independent of the models. Their values are smaller for hemoglobin than for myoglobin[6] and the distribution is wider for myoglobin, showing that it has a larger number of conformational substates. The three models studied reproduce well the experimental curves of 100K, 140K and 180K.

Keywords: Hemoglobin; reassociation dynamics; rebinding models.

INTRODUCTION

Myoglobin (Mb) and hemoglobin (Hb) have been extensively studied as models for proteins. Lately[1,2] a great number of dynamical studies have been performed concerning mainly the reaction of different ligands with Mb, in order to understand the oxygenation process. The studies at low temperatures ($T < 200K$) are important because they show the last step in the ligand-protein reaction namely the process of fixation of the ligand at the heme iron. At higher T, when several steps are present, the fixation process of the ligand at the iron may be the one which controls the reaction[3].

One of the first papers in this line and one which is basic for the following papers is by Austin et al.[4] In their experiment rebinding of photodissociated carbon monoxide in Mb has been observed in the temperature range between 40 and 350K. To interpret the data obtained, they assumed that the dissociated ligand encounters, on its way between the solvent and the ferrous heme iron four potential barriers in succession. The results in the range between 40 and 160K showed that $N(t)$, the fraction of non reassociated ligand in a time range 10^{-9} to 10^{-1} seconds, can not be described by an exponential function. To explain this behaviour the model (here called Model A) proposes the existence of conformational substates (CS) with different barrier heights for the transition from unbound state B to bound state A. At temperatures T higher than the freezing temperature T_g (about 200K), each protein molecule changes rapidly among the different substates, varying continuously its structure. At $T < T_g$ it remains in one particular conformational substate. In this tem-

perature range the ligand overcomes one single barrier E_{BA} in its reassociation process with the iron. E_{BA} is slightly different for each one of the molecular conformations, resulting, for $T < T_g$, in a temperature independent energy distribution $g(E)$. $g(E)$ is then the probability to find a protein with energy barrier between E_{BA} and $E_{BA} + dE_{BA}$ and is defined as $g(E_{BA})\ dE_{BA}$. $N(t)$ becomes

$$N(t) = \int g(E_{BA})\ \exp(-kt)\ dE_{BA} \qquad (1)$$

where k is the reaction rate which, at $T > 40K$, obeys the Arrhenius equation

$$k_{BA}(T) = A\ \exp(-E_{BA}/RT) \qquad (2)$$

where A is a frequency factor and R(=1.99 cal/mol.K) the gas constant.

Other models based on model A followed and different forms of the energy distributions g(E) were proposed. Two of them, by Agmon and Hopfield (model B)[5] and Young and Bowne (model C)[6], treat the problem from a microscopic point of view. Both models assume that the conformational substates follow a Boltzman distribution, resulting in an energy distribution g[E(x)], where x is the conformational coordinate of protein which parametrizes each CS. The total potential of the protein has contributions from the reaction potential V(r), where r is the Fe ligand distance and from the conformational potential V(x) which describes the fluctuations among the protein substates. The dif

ferences between these two models are: in model B V(x) is harmonic and the conformational stiffness is independent of the protein states; and in model C, V(x) is unharmonic and the conformational stiffness depends on each protein state.

The model A assumes that, in the case of Mb, in the temperature range between 40 and 160K, g(E) is temperature independent. The process is ligand-concentration independent since the ligand remains inside the heme pocket. When the temperature T is higher than T_g and the ligand moves away from Fe toward the solvent, other processes become important.

Carp hemoglobin rebinding with carbon monoxide (CO) was observed by Cobau et al.[7] in R (relaxed) and T (tense) states. Only the model B was applied to these results. They found significantly different parameters between these states.

In this work we apply models A and C to their experimental results for R state at 100, 140 and 180K. We verified that these models are as good as the model B in fitting the experimental curves at 180K.

We also noticed that the values of the frequency factor A and the value of the peak energy E^P are almost independent of the models.

None of the models here presented can be considered to be better than the others because:

1) - the experimental measurements are restricted to temperatures close to T_g;
2) - the three models involve many parameters;
3) - the models are distinguished one from the other by their distribution function g(E). The experimental results

give N(t) which is not a direct measurement of g(E). The integral evaluated with (eq. 1) to obtain N(t) is to be compared with the different models.

The second section describes the three models and the third one gives the results and discussion. In the Appendix we show the sensitivity of the reassociation curves and of the distribution functions to the parameters of each model.

MODELS

The model A determines a distribution function $g(k_{BA})$, for $T < Tg$, in terms of k_{BA} by the inverse Laplace transform. To determine $g(k_{BA})$ in terms of E_{BA} the observed rebinding function N(t) is approximated by a power law

$$N(t) = (1+t/t_o)^{-n} \qquad (3)$$

which describes reasonably well the observed curves over a fair range in time. n and t_o are temperature dependent parameters which give the slope of N(t) in the "straight" part of the logN(t)X logt plot, and the time at which N(t) breaks away from the horizontal, respectively.

The parameters n and t_o are determined at each temperature fitting N(t) curves by eq. (3).

The values of n and t_o chosen to calculate the distribution function $g(E_{BA})$, at $T < T_g$, are the ones which best fit the data points between 40 and 160K. Then

$$g(E_{BA}) = \frac{(At_o)^n}{RT\Gamma(n)} \exp\left[-\frac{nE_{BA}}{RT}\right] \qquad E_{BA} < E_{BA}^{max} \tag{4a}$$

$$g(E_{BA}) = 0 \qquad E_{BA} \geq E_{BA}^{max} \tag{4b}$$

If $g(E_{BA})$ is temperature independent eq. (4a) can be written

$$g(E_{BA}) = \beta \exp(-\alpha E_{BA})$$

where α and β are constants. Comparison of equations (4) and the equation above shows that n satisfies the relation

$$n = \alpha RT \tag{5}$$

where T is the experimental temperature.

As a result, $g(E_{BA})$ can take the form given by Alberding et al.[8]

$$g(E_{BA}) = g_o\{\exp[\alpha(E_{BA}^P - E_{BA}) - n \exp \frac{\alpha}{n}(E_{BA}^P - E_{BA})]\} \tag{6}$$

where E_{BA} is the energy corresponding to the maximum value of the distribution $g(E_{BA})$ and g_o is the normalization constant. The calculated N(t) are fitted from eq. (1) with log(A), E^P, α and n as adjustable parameters.

In the model B the activation energy is determined by the intersection of two potential surfaces of B (unbound) and A (bound) states, $V_B(r,x)$ and $V_A(r,x)$, respectively. In the state A the heme iron has zero spin, and $V_A(r)$ is a Morse curve; in the state B, the spin is 2 and $V_A(r)$ is repulsive. V(x) is har-

monic with the conformational stiffness independent of the binding state of protein, either A or B.

The distribution function g[E(x)] suggested by this model is

$$g[E(x)] = \left|\frac{2E}{D} - 3\right| \frac{1}{fx_o}\left(\frac{f}{2\pi RT_g}\right)^{1/2} \exp\left[-\frac{1}{2RT_g}(x-x_o)^2\right] \tag{7}$$

where the conformational coordinate x is related to the activation energy E_{BA} by

$$x = \frac{x_o}{2} + \frac{\Delta}{fx_o} - E\left(3 - \frac{E}{D}\right)\frac{1}{fx_o} \tag{8}$$

Besides the frequency factor A, the adjustable parameters are (see fig. 3 from ref. 5): D, the depth of the reaction well; Δ, the shift between V_B and the surface of zero potential; f, the conformational stiffness; and x_o, the difference of the coordinate x between the two spin states of the protein in equilibrium. Below T_g the protein no longer overcomes the barrier between the substates and remains frozen in a particular substate. The population at $T < T_g$ is a non-equilibrium population characteristic of the freezing temperature T_g which is assumed equal to 200K.

Since $E/D << 3$, g[E(x)] given by eq. (7) can be considered approximately a gaussian.

In the third model, V(x) is unharmonic and the conformational stiffness is characteristic for A,B and transition states. The energy barrier does not depend on the form of V(r), but

is determined as the difference between the protein potential in the activated state and the unbound-B state. The transition between conformational substates are described by the conformational potential $V_c^i(x)$ where i=A,B or ‡ (transition state). Because of the large number of substates, $V_\nu^i(x)$ is a continuous function of x. Assuming that the conformational energy is isotropic, it can be expressed as follows

$$V_\nu^i(x) = f_i\, x^{1/\nu} + V_\nu^i(0)$$

where $x >> 0$.

The barrier height is

$$E_{BA} = E_{BA}(x) = E_{min} + (f^{\ddagger} - f_B)\, x^{1/\nu}$$

This equation assumes that the protein coordinate x does not change during the B → A transition.

Model C assumes a Boltzman distribution for the population of the CS, and for $T < T_g$ this distribution is temperature independent and is determined for $E_{BA} \geq E_{min}$ as follows

$$g(E_{BA}) = g(E_{BA}, T_g)$$

$$= C_f (E_{BA}-E_{min})^{3\nu-1} \exp[-\alpha_f (E_{BA}-E_{min})] \qquad (9)$$

with

$$C_f = \frac{\alpha_f^{3\nu}}{\Gamma(3\nu)}$$

and

$$\alpha_f = f_A/(f^{\ddagger}-f_B)\ R\,T_g$$

E_{min} is defined as the smallest activation energy of a conformational substate such that the protein coordinate x is zero.

The four adjustable parameters in this model are: A, ν, E_{min} and α_f.

RESULTS AND DISCUSSION

In the present work we fit the curves of reassociation of CO with carp Hb in R state, using the least-squares fit method[9] and the Monte Carlo method which minimizes the mean square error.

Since the parameters in the model A which fit the curves at 140K do not reproduce well the curves taken at others temperatures, the fits have been made for theoretical values of log[N(t)] at 100K. N(t) is given by eq. (1) with g(E) corresponding to each model. This suggests that the hypothesis that the distribution g(E) is temperature-independent and that the ligand reassociation is made across one single potential barrier near the iron, can not be valid anymore. We verify the existence of several sets of parameters which fit well the curves at 100K, but we present in Tables I, II e III the set which gives the best fit simultaneously at the three temperatures, supposing that g(E) is temperature independent at $T < T_g$.

Table I gives a comparison between the values of the parameters from model B obtained in this work and the ones given in ref. 7, where the value of the frequency factor which appears in eq. (2) is not given. The last two lines of Table I show the peak energy E^P and the minimum energy E_{min} of the distribution g(E) found by the five parameters fitting. These energies are adjustable parameters in the models A and C, respectively.

Fig. 1 gives the curves that correspond to the set of parameters shown in Table I, where the dashed lines are the results in ref. 7 and the solid lines are our results. We can clearly see that our fit is better than the one in ref. 7. However, there is only a deviation of about 7% between the two sets of parameters.

This result can be understood because our value for x_o is almost the same as in ref. 7. This quantity defines the shape of the curve. Δ and f influence the curve, too, but to a smaller degree. The frequency factor A does not change the shape of the N(t) curve but influences its absolute value. The absolute value of N(t) depends equally on A, Δ and x_o variations, and to a lesser degree on f, in the range of the values presented in Table I. The fit based on this model is insensitive to parameter D, both in the form and in the absolute value of N(t).

Table II shows the results obtained applying model C, remembering that in this model the peak energy E^P is not an adjustable parameter, but is determined from the distribution g(E). The corresponding plot log N(t) X log t is shown in fig. 2.

The curvature is defined by α_f and ν which also determine the peak energy. The absolute value of N(t) is more sensitive to parameter A, and almost insensitive to E_{min}.

Table III shows two sets of parameters of model A.

In the set A.1 we consider log(A), E^P, n and α as independent parameters, that is to say, without taking into account eq. (5), which relates n and α. To satisfy this equation T must be about 515K, a surprisingly high value. This result can not be interpreted as in ref. 4, where, for Mb, in the range from 40 to 160K, the chosen n and α are related by eq. (5) at the temperature of the best fit, T = 120K. The fitting was made with the value of T^* between 100 and 220K. So that the temperature T^* which connects α and n in eq. (5), be of the order of T_g. The set A.2 was obtained with independent E^P, n and T^* and log(A) was fixed at a value equal to the mean value of log (A) found using the models A.1, B and C.

The curves of N(t) corresponding to both sets are shown in fig. 3. We can observe that both reproduce well the experimental data with some difference in the behaviour at the end of the curves.

The curvature in this model is mainly defined by the parameter α but it is also weakly affected by n. The value of N(t) is influenced, basically, by the frequency factor A, but is also sensitive to E^P. The minimum energy, E^{min}, is determined by E^P and n.

In spite of the great difference in the values of the parameters n and α (consequently in E_{min} and T^*) between the A.1 and A.2 sets, we can not choose one of them as the set that

best reproduces the available experimental results. The figures 1-3 show that the fits at 100 and 140K are better than at 180K. This fact gives an additional support for the supposition that near T_g ($\sim$200K), the distribution function g(E) is not temperature independent anymore, and that other reaction mechanisms, can give contribution to N(t).

The Table IV shows the comparison between the quantities common to the three models.

Table IV and fig. 4 show that the models can be distinguished one from another by the different values either of the minimum energy or of the distribution width λ. Model A.2 has $E_{min} \neq 0$ significantly different from the E_{min} of the other models. However it is in model C that this quantity is defined "a priori", although we have obtained a very small value for it (0.4kcal/mol). For Mb, Young[6] considers that the gaussian distribution[5] (model B) does not give a good fit for the reassociation of CO with Mb, mainly because it has a significant contribution for values of $E_{BA} < E_{min}$. Our results suggest that the minimum energy does not determine the best model for Hb since the four distributions obtained, give good fits, independently of the value of E_{min}. Even with distribution with small E_{min} (value of the energy smaller than the value found in model A.2) we can obtain fits as good as the ones in figs. 1 and 2. The observation that the N(t) curve is weakly sensitive to variations of E_{min} strengthens this supposition.

The distribution width does not determine which is the best model either. In fig. 4 we see that the distribution in model A.2 has a width very different from the others, but this is not enough to determine if this model is the best. Although

the tail of the curve obtained from model A.2 has a different behaviour, in this region the signal to noise ratio is too low to allow for a choice between the two fits.

In Table IV we see that the values of E^P and A are almost the same for all the models. In view of this we consider that the two quantities are the most relevant to the fitting.

For all the models discussed here, these two parameters, A and E^P, are smaller for Hb than for Mb[6], and the distribution g(E) for Mb is wider than for Hb, showing that Mb has a greater number of conformational substates.

This work shows that the models proposed to understand the reassociation of CO with Mb can be also utilized for Hb, in spite of Hb being a protein composed of four chains with cooperative effect in the Fe-ligand reaction. It would be interesting to make a comparative study of these models for Hb in a larger temperature range, mainly in the region below 100K.

APPENDIX

We show in this section the behaviour of the distribution function g(E) and of the reassociation curves logN(t)X logt as a function of changes of only one parameter of each model.

Some parameters affect only the absolute value of the curves and other modify its curvature.

We verified that the shape of the curve does not change when different values of the same parameters yield curves which can be superposed by a simple shift. If such superposition is not possible it is because the curvature has changed.

Only the frequency factor A is common to the three models and does not affect the shape of the curve but strongly modifies its intensity. The distribution functions do not depend on A.

The solid lines in the following figures represent the curves obtained from the best fits. Other curves on the same figure show the effect of the variation of the parameters which most strongly affect the curves in each model. The variation utilized is about 30% of the value of the parameters used for the solid lines.

The effect of the parameters on the logN(t) X logt curves is described in the text and can be infered from the curves in figures 5-c, 6-b and 7-b.

FIGURE CAPTIONS

Fig. 1 - Rebinding of CO to carp-Hb, in R state, using model B. Solid lines: our results. Dashed lines: results from ref. 5. Values of parameters taken from Table I.

Fig. 2 - Rebinding of CO to carp-Hb, in R state, using model C. Values of parameters are taken from Table II.

Fig. 3 - Rebinding to CO of carp-Hb, in R state, using model A. Values of parameters are taken from Table III. Solid lines: set A.1. Dashed lines: set A.2.

Fig. 4 - Energy distributions g(E) for the three models ··· model A.1. — model A.2. --- model B. -·- model C.

Fig. 5-a- g(E) for model A.1. Solid lines: parameters from Table III. ---E^P = 2.47 kcal/mol; -·-α = 3.64 mol/kcal; ···n=3.64.

Fig. 5-b- g(E) for model A.2. Solid lines: log(A)=8.7; E^P = 1.9kcal/mol; n=0.6; α = 2.01 mol/kcal and T^* = 150K. Dashed lines: α = 1.55 mol/kcal and T^* = 195K.

Fig. 5-c- Reassociation curves for model A. The values of the parameters are the same as in Fig. 5-a.

Fig. 6-a -g(E) for model B. Solid lines: parameters from Table I. ···Δ=13.39 kcal/mol; -·-f=15.86 kcal/(mol a.u.^{2}) and --- x_o=1.13 a.u. Obs: The value of the parameter D almost does not affect the curves.

Fig. 6-b - Reassociation curves for model B. The values of the parameters are the same as in Fig. 6-a.

Fig. 7-a- g(E) for model C. Solid lines: parameters from Table II. --- E_{min}=0.52 kcal/mol; ···ν=2.86 and -·-α_f=5.2 mol/kcal.

Fig. 7-b - Reassociation curves for model C. The values of the parameters are the same as in Fig. 7-a.

ACKNOWLEDGEMENTS

Three of the authors would like to show their appreciation to the Conselho Nacional de Desenvolvimento Científico e Tecnológico for the fellowships received during this work.

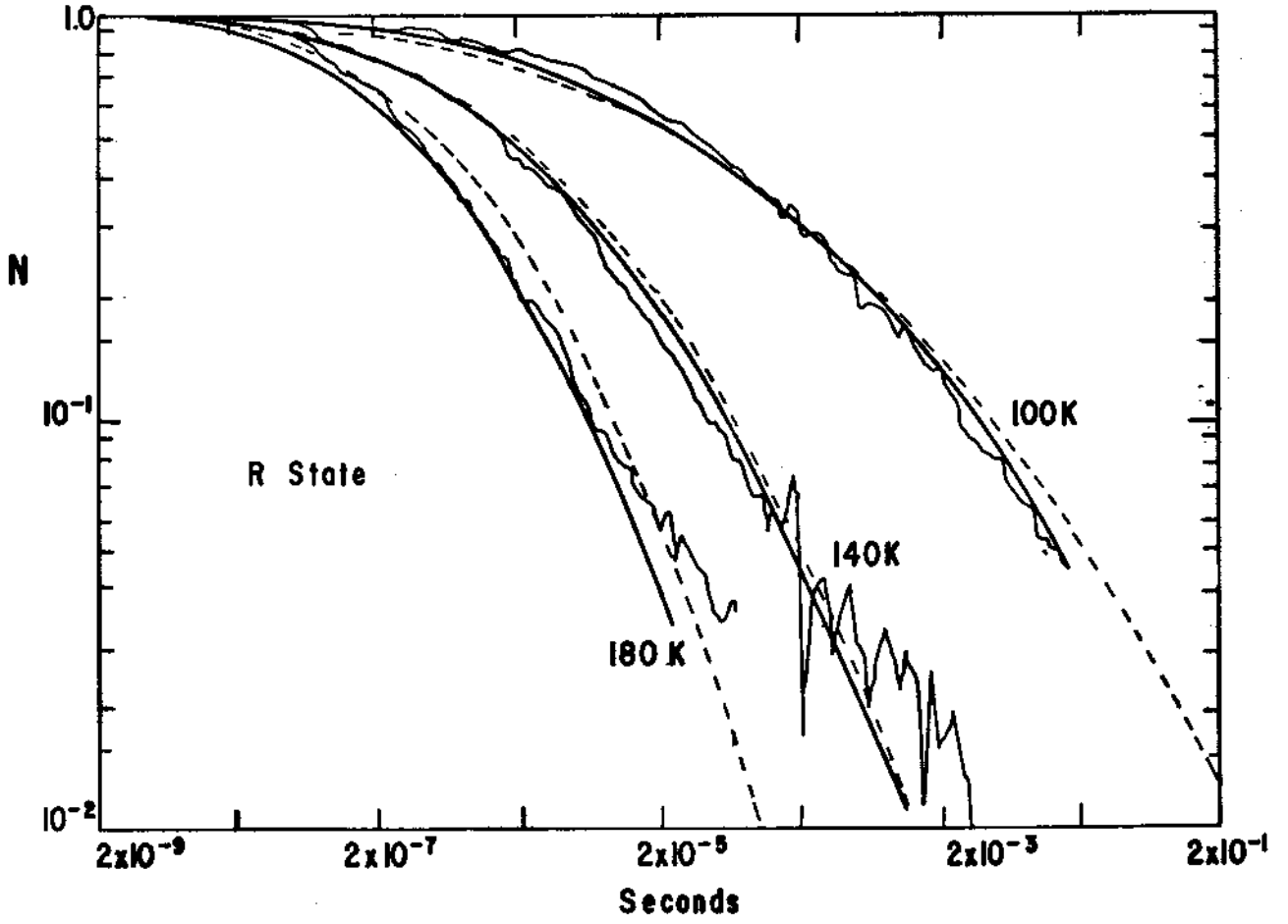
1.0
N
10^{-1}
10^{-2}
R State
100K
140K
180 K
$2x10^{-9}$
$2x10^{-7}$
$2x10^{-5}$
$2x10^{-3}$
$2x10^{-1}$
Seconds

Fig. 1

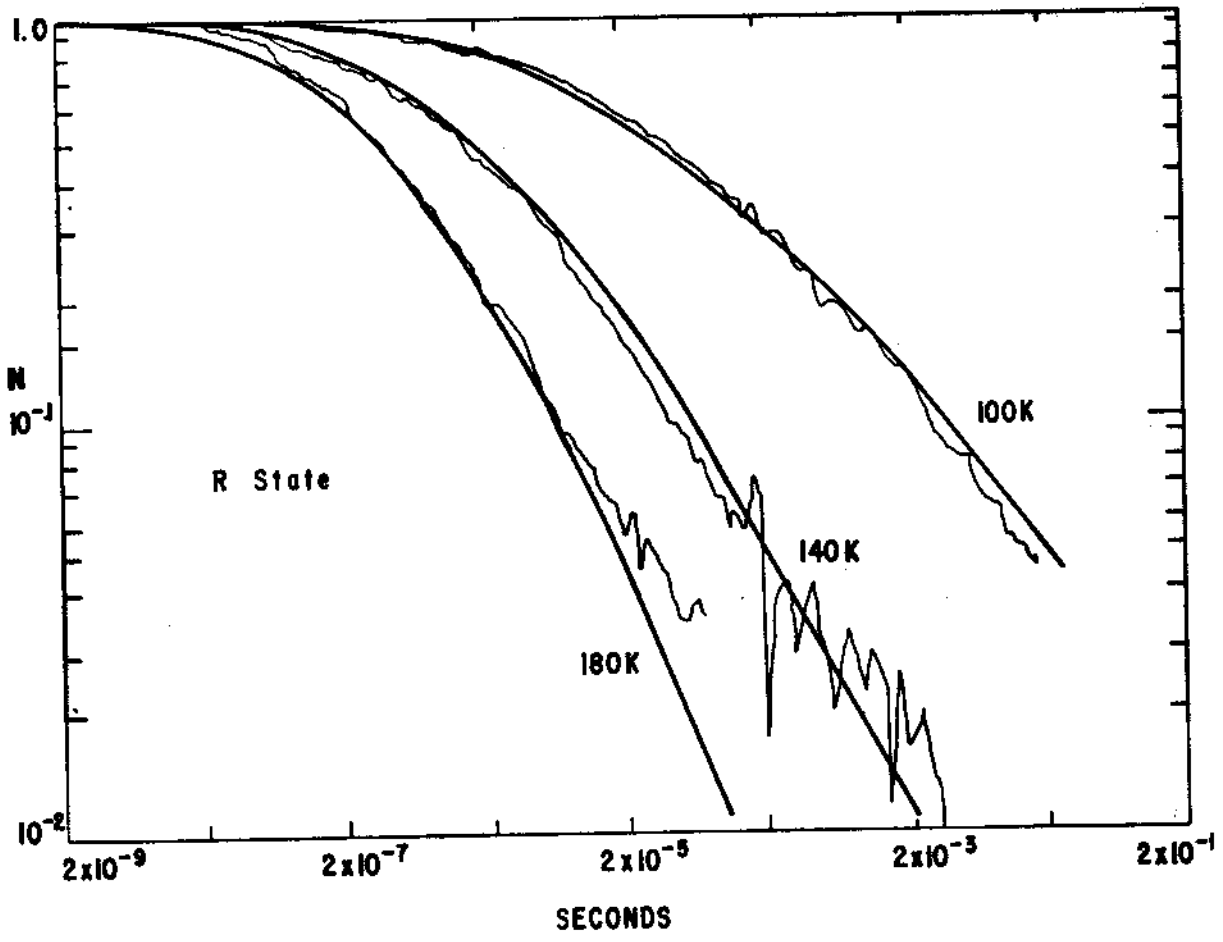
1.0
N
10^{-1}
10^{-2}
R State
100K
140K
180K
$2x10^{-9}$
$2x10^{-7}$
$2x10^{-5}$
$2x10^{-3}$
$2x10^{-1}$
SECONDS

Fig. 2

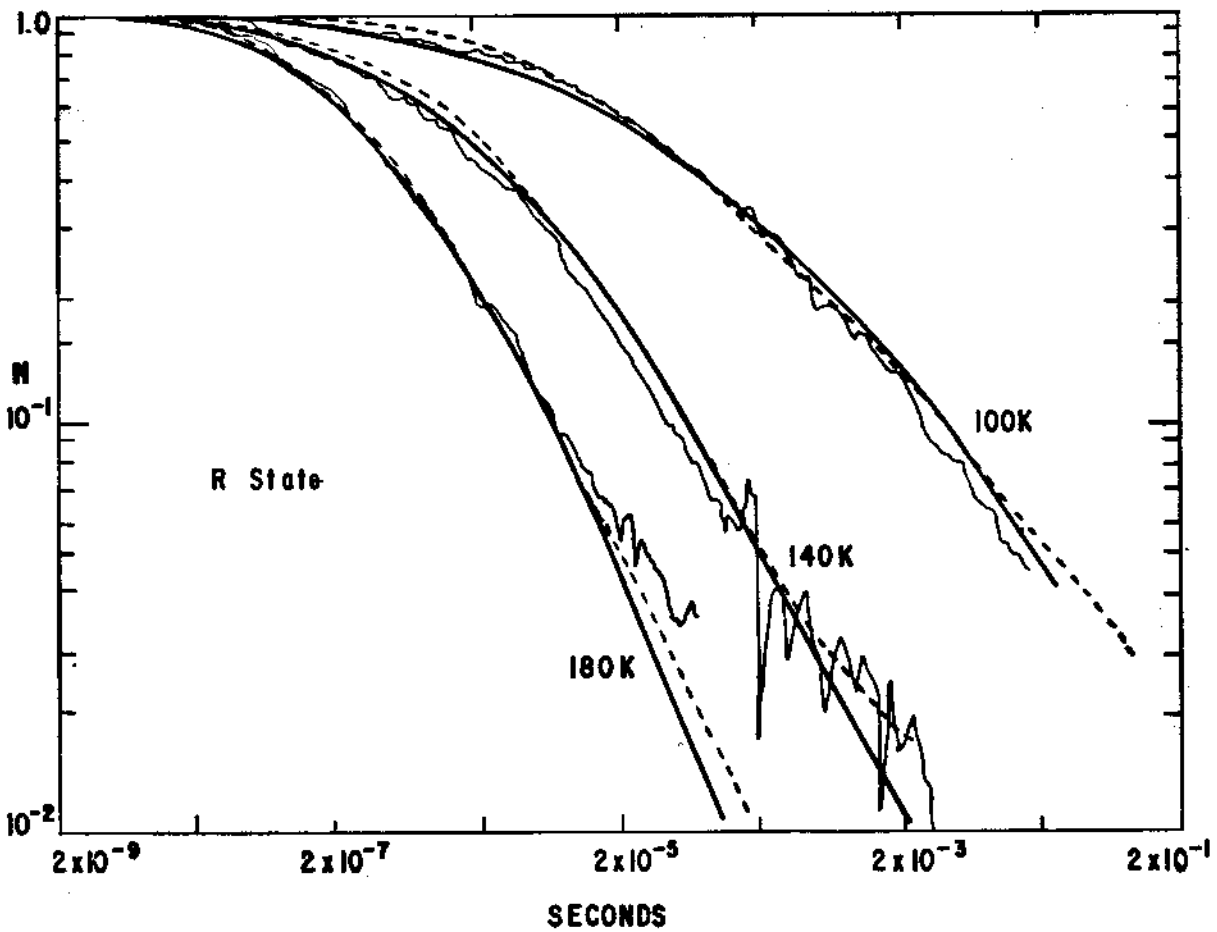
1.0
M
10^{-1}
10^{-2}
R State
100K
140K
180K
$2x10^{-9}$
$2x10^{-7}$
$2x10^{-5}$
$2x10^{-3}$
$2x10^{-1}$
SECONDS

Fig. 3

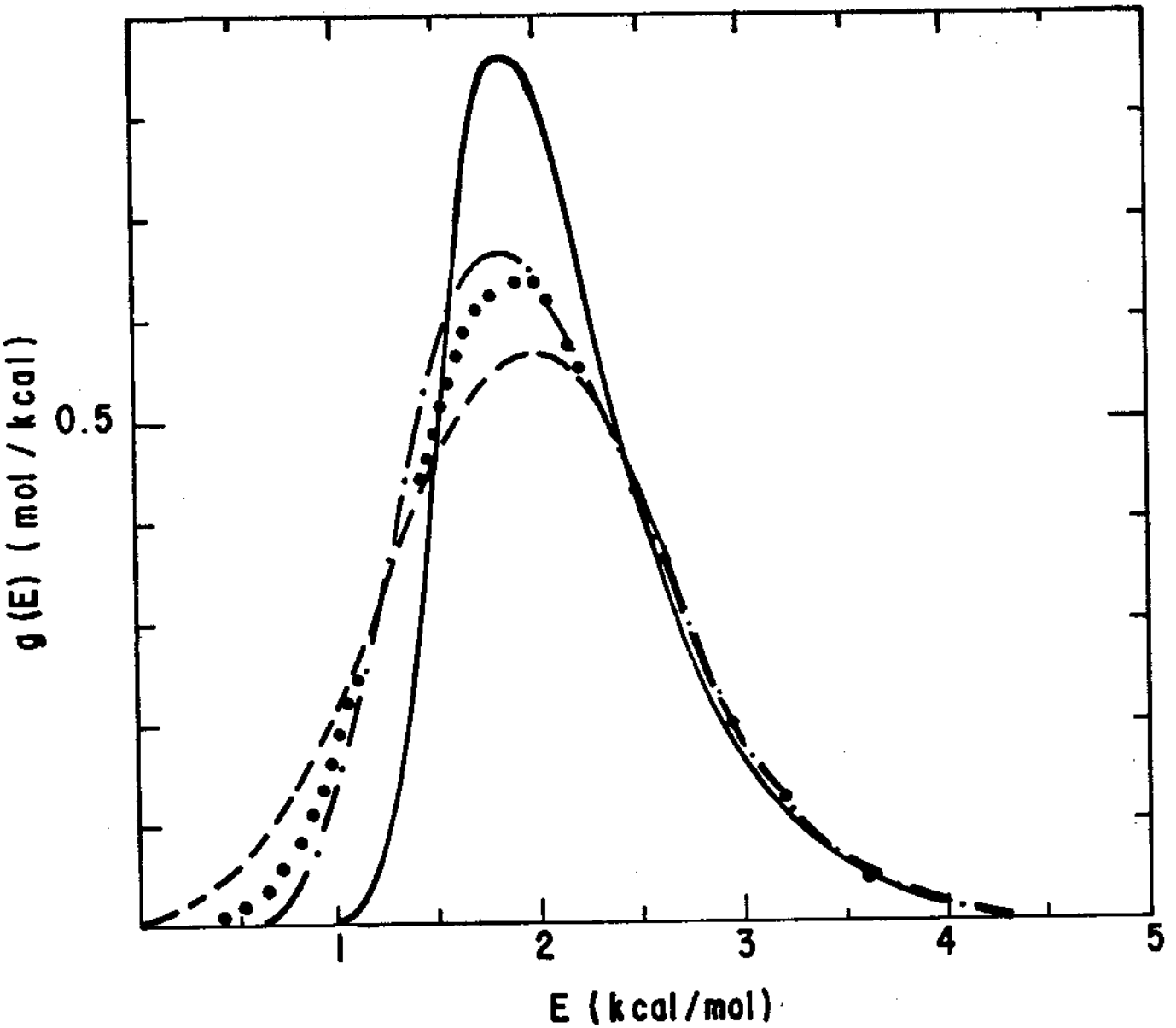

Fig. 4

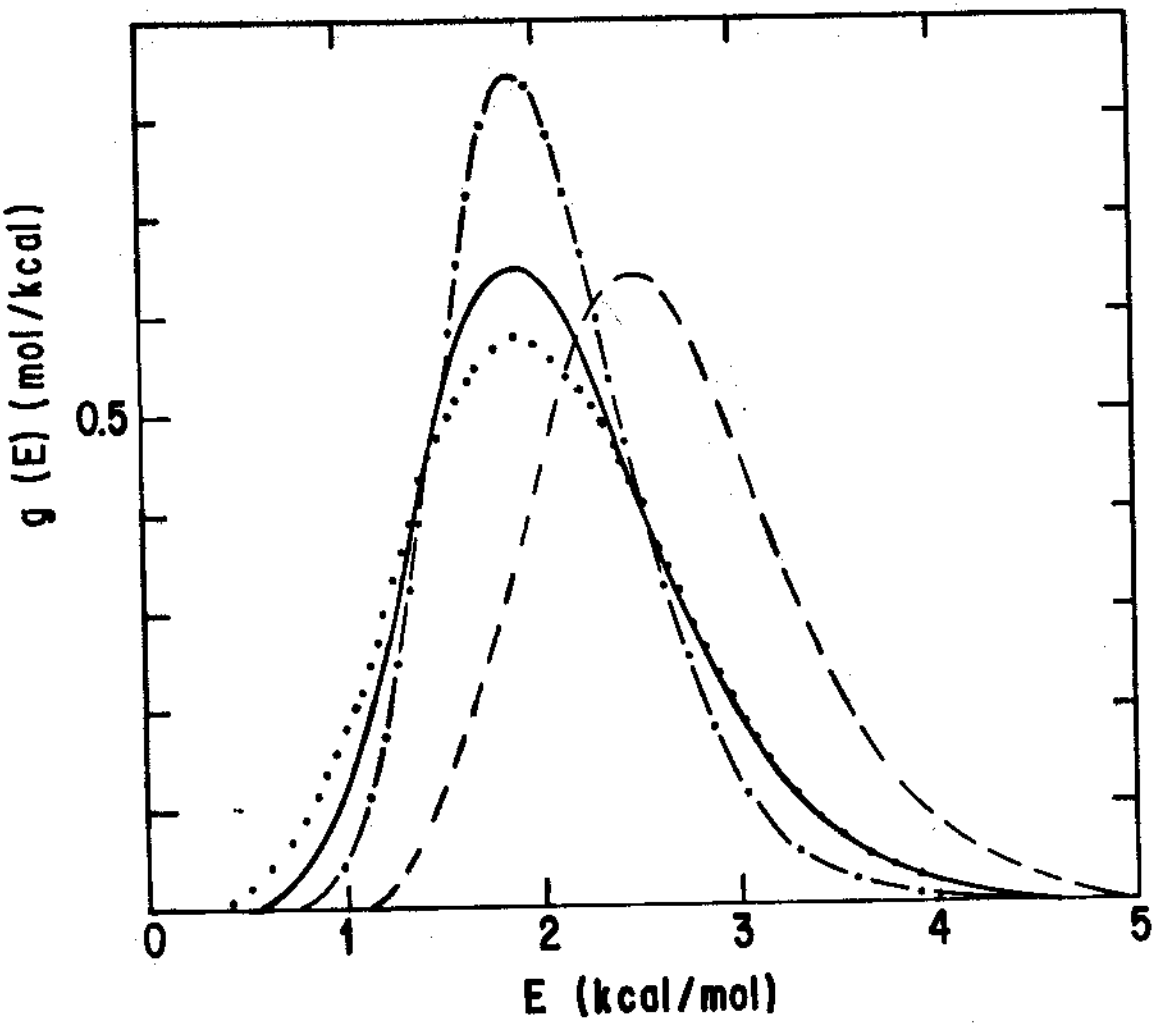

Fig. 5-a

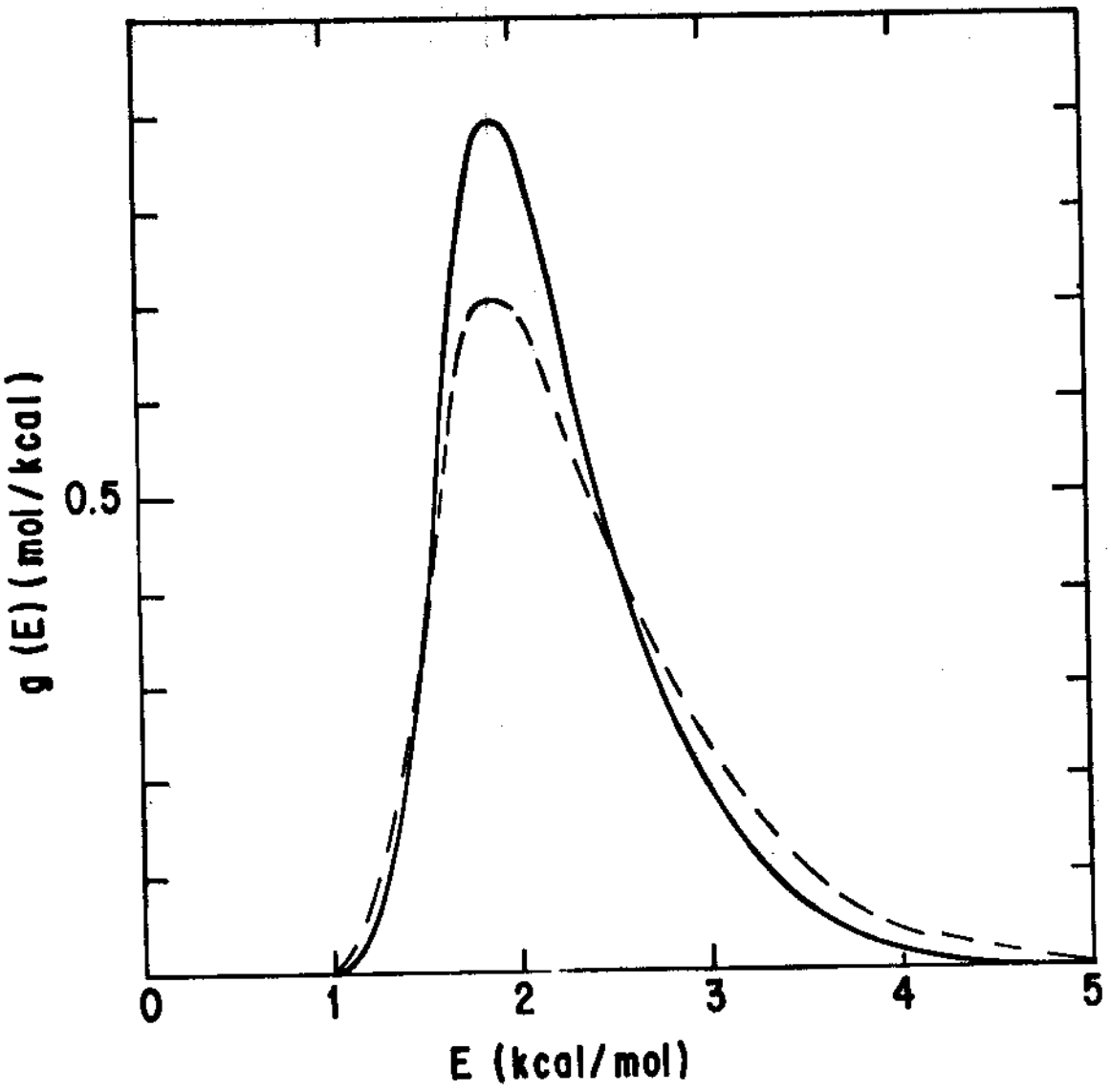

Fig. 5-b

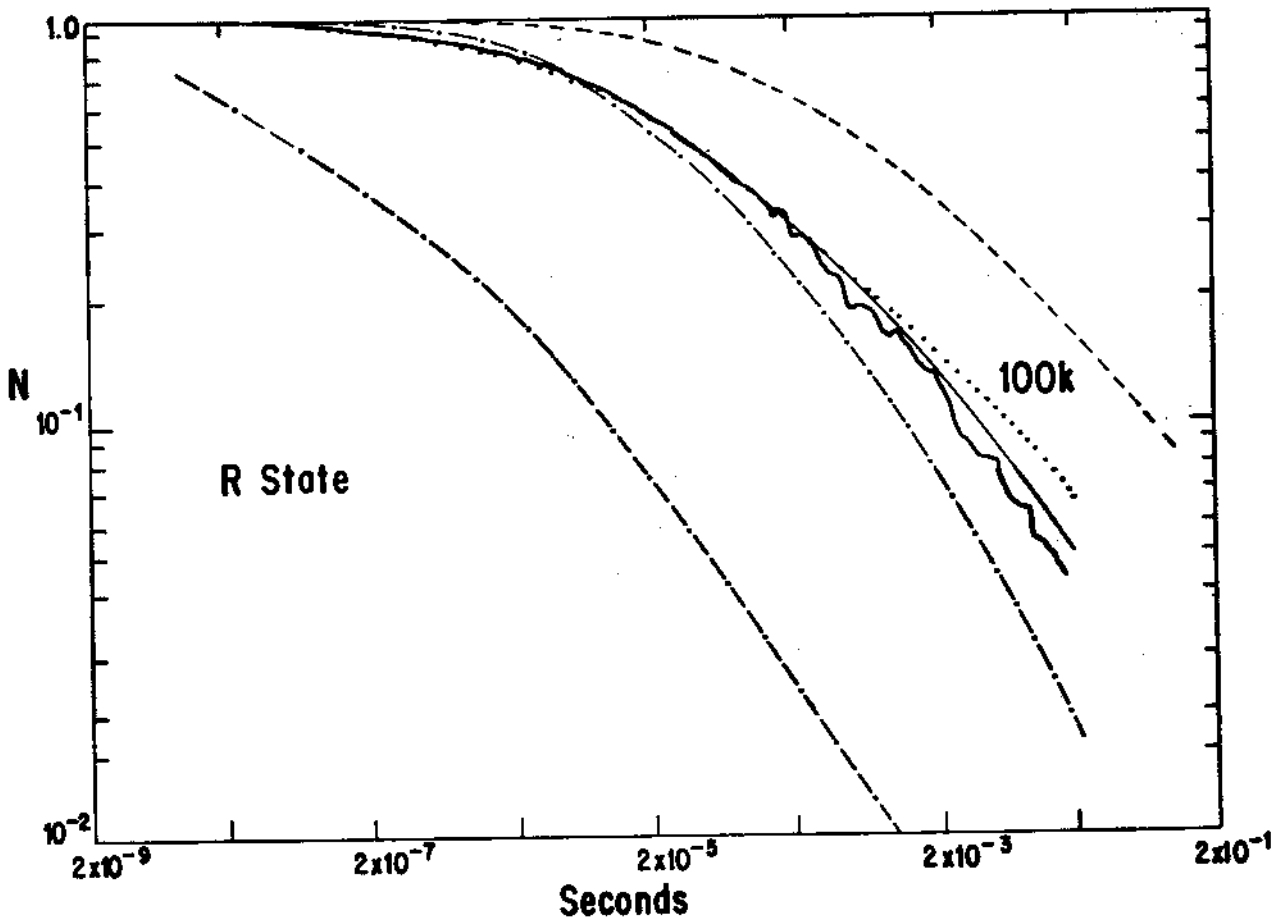
1.0
N
10^{-1}
10^{-2}
R State
100k
$2x10^{-9}$
$2x10^{-7}$
$2x10^{-5}$
$2x10^{-3}$
$2x10^{-1}$
Seconds

Fig. 5-c

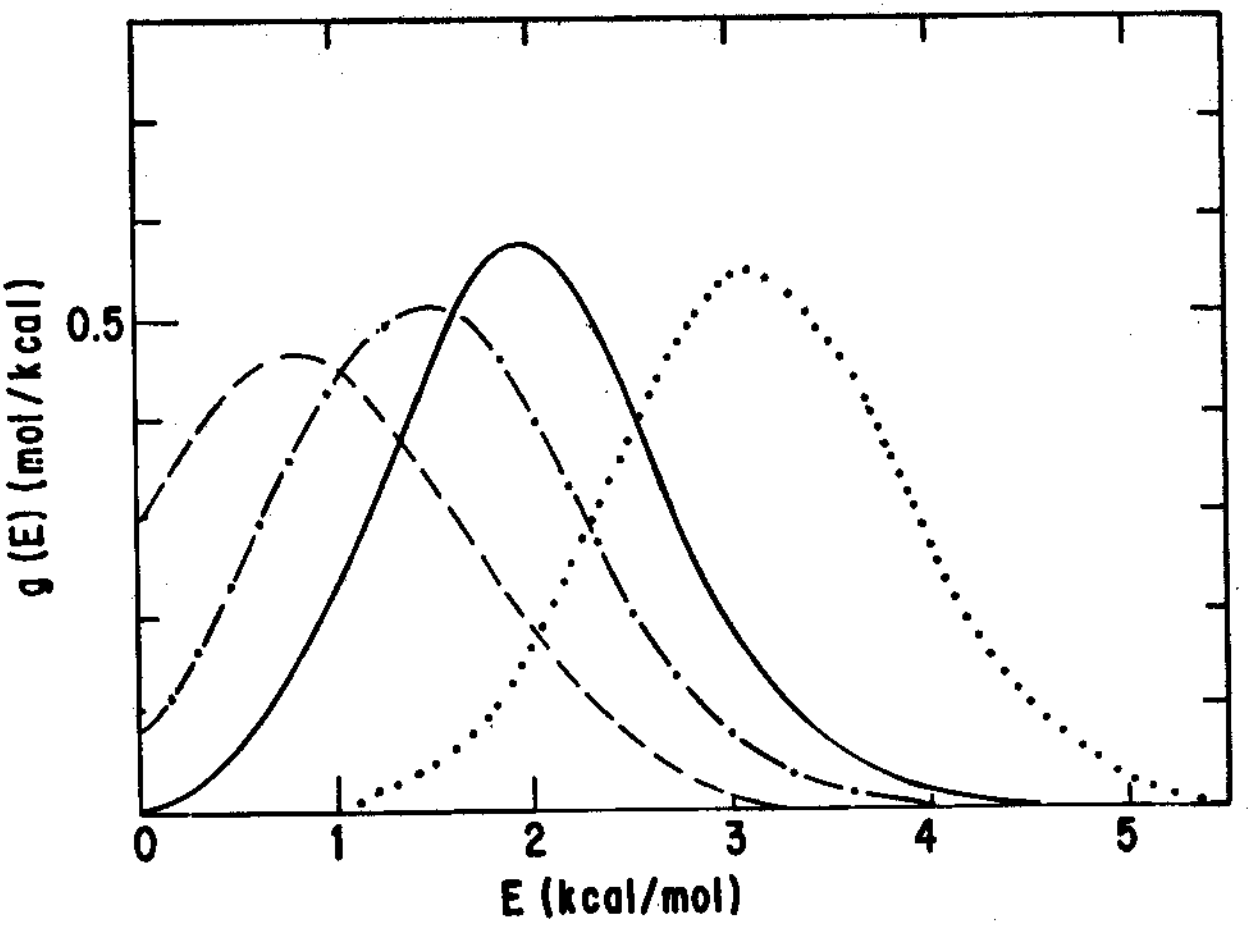

Fig. 6-a

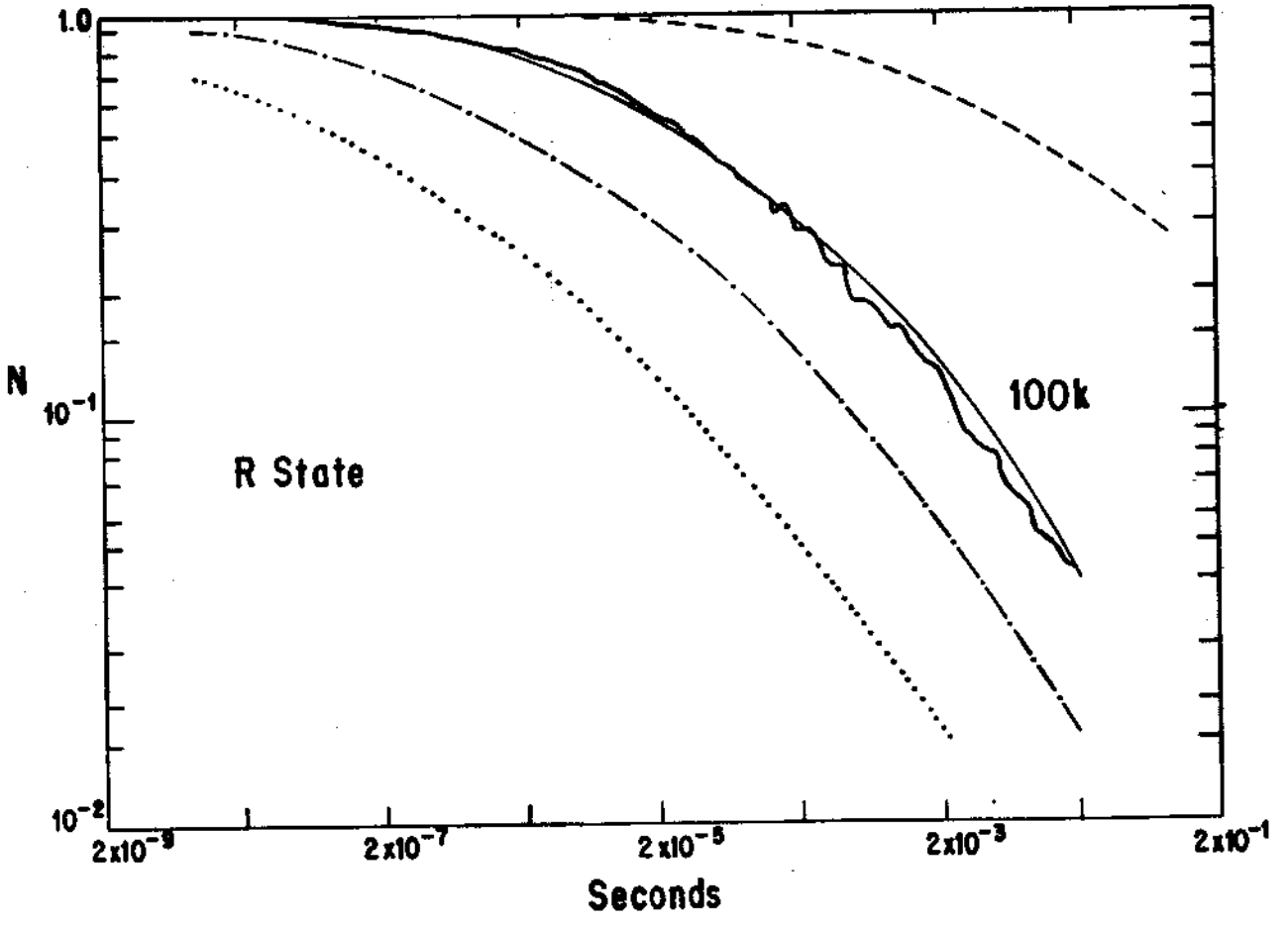
1.0
N
10^{-1}
10^{-2}
R State
100k
$2x10^{-9}$
$2x10^{-7}$
$2x10^{-5}$
$2x10^{-3}$
$2x10^{-1}$
Seconds

Fig. 6-b

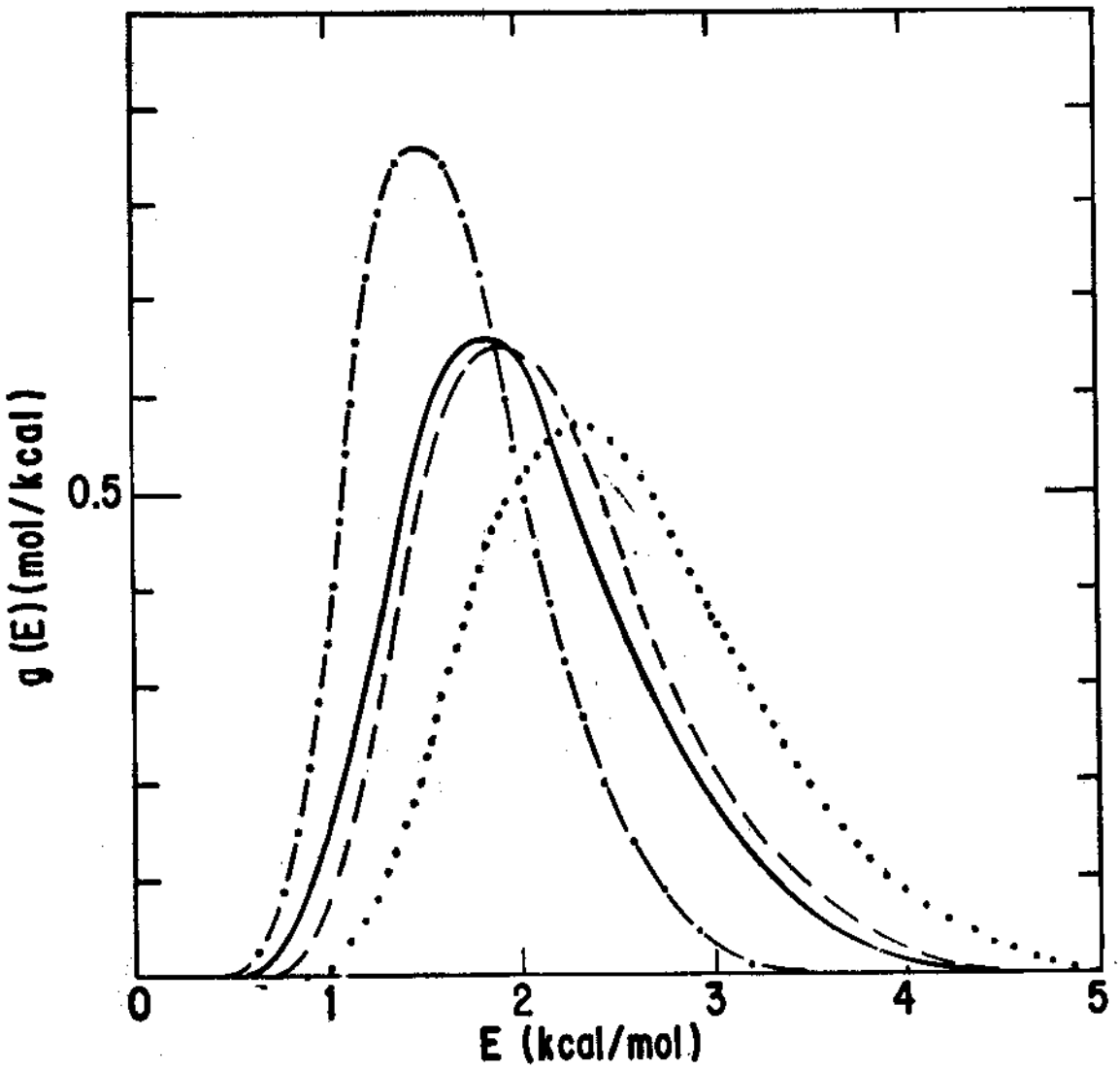

Fig. 7-a

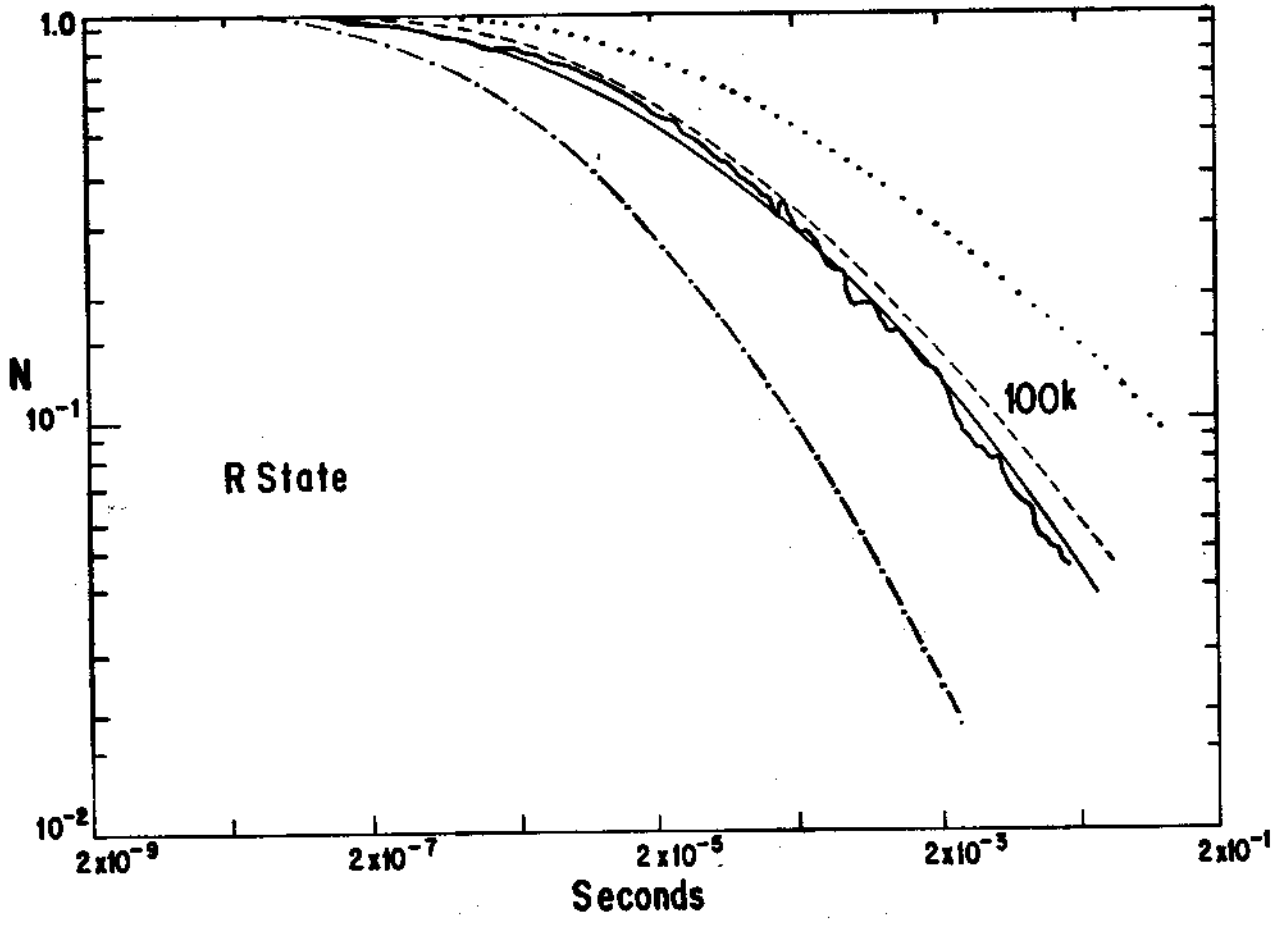
1.0
N
10^{-1}
10^{-2}
R State
100k
$2x10^{-9}$
$2x10^{-7}$
$2x10^{-5}$
$2x10^{-3}$
$2x10^{-1}$
Seconds

Fig. 7-b

TABLE I - Parameters for model B for rebinding of CO in Carp-Hb in R state.

MODEL B[5]		
	Our results	Ref. 7
$\log[A(s^{-1})]$	8.6	----
D(kcal/mol)	15.2	16.0
Δ(kcal/mol)	10.3	9.7 + 0.4
f(kcal/mol.a.u.^{2})	12.2	13.0 + 0.6
x_o(a.u.)	0.87	0.88 + 0.1
E^p(kcal/mol)	2.0	1.6
E_{min}(kcal/mol)	0.0	0.0

TABLE II - Set of parameters for model C.

MODEL C^6	
$\log[A(s^{-1})]$	8.7
E_{min}(kcal/mol)	0.4
α_f(mol/kcal)	4.0
ν	2.2
E^p(kcal/mol	1.8

TABLE III - Sets of parameters for model A obtained by the fitting of log N(t) at 100K. The independent parameters are: set A.1: log(A), E^P, α and n; set A.2; E^P, n and T^*.
This value corresponds to the mean value of log(A) using the three models.

MODEL A^4		
	A.1	A.2
$\log[A(s^{-1})]$	8.7	8.7##
E^P(kcal/mol)	1.9	1.8
n	2.8	0.6
α(mol/kcal)	2.8	1.9
T^*(K)	515.	158.
E_{min}(kcal/mol)	0.4	1.

TABLE IV - Comparison of the results obtained in this work for the three models.

		log(A)	E^P	E_{mim}	λ	g(E)
		A(s^{-1})	kcal/mol			mol/kcal
MOD.A[4]	A.1	8.7 #	1.9	0.4	1.5	0.64
	A.2	8.7	1.8	1.	1.	0.86
MOD.B[5]		8.6	2.0	0.	1.6	0.66
MOD.C[6]		8.7	1.8	0.4	1.4	0.67

References

1 a) Gibson, Q.H. J. Physiol. 1956, *134*, 112.

b) Antonini, E. and Brunori,M. "Hemoglobin and Myoglobin in Their Reactions with Ligands", Amsterdam, North-Holland Co. (1971).

c) Austin, R.H., Beeson, K.N., Eisenstein, L., Frauenfelder, H., Gunsalus, I.C. and Marshall, V.P. Science 1973, *181*, 541.

d) Frauenfelder, H. Mossbauer Eff. Proc. Int. Conf. 5th. 1973, *401*.

2 Austin, R.H., Beeson, K.N., Eisenstein, L., Frauenfelder, H., Gunsalus, I.C. and Marshall, V.P. Phys. Rev. Lett. 1974, *32*, 403.

3 Ansari, A., Dilorio, E.E., Dlott, D.D., Frauenfelder,H., Iben,I.E.T., Langer, P., Roder, H., Sauke, T.B. and Shyamsunder, E. Biochemistry 1986, *25*, 313.

4 Austin, R.H., Beeson, K.W., Eisenstein, L., Frauenfelder, H. and Gunsalus, I.C. Biochemistry 1975, *14*, 5355.

5 Agmon, N. and Hopfield, J.J. J. Chem. Phys. 1983, *79(4)*, 2042.

6 Young, R.D. and Bowne, S.F. J. Chem. Phys. 1984, *81(8)* 3730.

7 Cobau, W.G., Legrange, J.D. and Austin, R.H. Biophysics J. 1985, *47*, 781.

8 Alberding, N., Chan, S.S., Eisenstein, L., Frauenfelder, H., Good, D., Gunsalus, I.C., Nordlund, T.M., Perutz, M.F., Reynolds, A.H. and Sorensen, L.B. Biochemistry. 1978, *17*, 43.

9 Bevington, P.R. "Data Reduction and Error Analysis for the Physical Sciences". 1969, McGraw-Hill, Inc.